




Two KTR Mannosyltransferases Are Responsible for the Biosynthesis of Cell Wall Mannans and Control Polarized Growth in *Aspergillus fumigatus*

Christine Henry,^a Jizhou Li,^a  François Danion,^{a,b} Laura Alcazar-Fuoli,^c Emilia Mellado,^c Rémi Beau,^a Grégory Jouvion,^d Jean-Paul Latgé,^a Thierry Fontaine^a

^aAspergillus Unit, Institut Pasteur, Paris, France

^bNecker-Enfants Malades Hospital, Department of Infectious Diseases and Tropical Medicine, Paris Descartes University, Paris, France

^cSpanish Network for Research in Infectious Diseases (REIPI RD16/0016), ISCIII, Majadahonda, Madrid, Spain

^dUnité de Neuropathologie Expérimentale, Institut Pasteur, Paris, France

ABSTRACT Fungal cell wall mannans are complex carbohydrate polysaccharides with different structures in yeasts and molds. In contrast to yeasts, their biosynthetic pathway has been poorly investigated in filamentous fungi. In *Aspergillus fumigatus*, the major mannan structure is a galactomannan that is cross-linked to the β -1,3-glucan-chitin cell wall core. This polymer is composed of a linear mannan with a repeating unit composed of four α 1,6-linked and α 1,2-linked mannoses with side chains of galactofuran. Despite its use as a biomarker to diagnose invasive aspergillosis, its biosynthesis and biological function were unknown. Here, we have investigated the function of three members of the Ktr (also named Kre2/Mnt1) family (Ktr1, Ktr4, and Ktr7) in *A. fumigatus* and show that two of them are required for the biosynthesis of galactomannan. In particular, we describe a newly discovered form of α -1,2-mannosyltransferase activity encoded by the *KTR4* gene. Biochemical analyses showed that deletion of the *KTR4* gene or the *KTR7* gene leads to the absence of cell wall galactomannan. In comparison to parental strains, the Δ *ktr4* and Δ *ktr7* mutants showed a severe growth phenotype with defects in polarized growth and in conidiation, marked alteration of the conidial viability, and reduced virulence in a mouse model of invasive aspergillosis. In yeast, the KTR proteins are involved in protein O- and N-glycosylation. This study provided another confirmation that orthologous genes can code for proteins that have very different biological functions in yeasts and filamentous fungi. Moreover, in *A. fumigatus*, cell wall mannans are as important structurally as β -glucans and chitin.

IMPORTANCE The fungal cell wall is a complex and dynamic entity essential for the development of fungi. It allows fungal pathogens to survive environmental challenge posed by nutrient stress and host defenses, and it also is central to polarized growth. The cell wall is mainly composed of polysaccharides organized in a three-dimensional network. *Aspergillus fumigatus* produces a cell wall galactomannan whose biosynthetic pathway and biological functions remain poorly defined. Here, we described two new mannosyltransferases essential to the synthesis of the cell wall galactomannan. Their absence leads to a growth defect with misregulation of polarization and altered conidiation, with conidia which are bigger and more permeable than the conidia of the parental strain. This study showed that in spite of its low concentration in the cell wall, this polysaccharide is absolutely required for cell wall stability, for apical growth, and for the full virulence of *A. fumigatus*.

KEYWORDS *Aspergillus fumigatus*, galactomannan, KTR, mannosyltransferase, biosynthesis, cell wall

Citation Henry C, Li J, Danion F, Alcazar-Fuoli L, Mellado E, Beau R, Jouvion G, Latgé J-P, Fontaine T. 2019. Two KTR mannosyltransferases are responsible for the biosynthesis of cell wall mannans and control polarized growth in *Aspergillus fumigatus*. mBio 10:e02647-18. <https://doi.org/10.1128/mBio.02647-18>.

Editor Bernhard Hube, Leibniz Institute for Natural Product Research and Infection Biology—Hans Knoell Institute Jena (HKI)

Copyright © 2019 Henry et al. This is an open-access article distributed under the terms of the [Creative Commons Attribution 4.0 International license](https://creativecommons.org/licenses/by/4.0/).

Address correspondence to Jean-Paul Latgé, jean-paul.latge@pasteur.fr, or Thierry Fontaine, thierry.fontaine@pasteur.fr.

This article is a direct contribution from a Fellow of the American Academy of Microbiology. Solicited external reviewers: Axel Brakhage, Hans-Knoell-Institute; Aaron Nieman, Stony Brook University; Dimitrios Kontoyiannis, University of Texas MD Anderson Cancer Center.

Received 29 November 2018

Accepted 12 December 2018

Published 12 February 2019

In fungi, mannans are composed of both short *O*- and *N*-linked mannans decorating glycoproteins and long mannan chains which are a major component of the fungal cell wall. *N*-linked and *O*-linked glycans have similar branched structures in yeasts and molds (1), and their synthesis follows the same pathway in yeasts and molds (2–6). In contrast, major differences have been found in the structural organization of the long mannans present in the cell wall of yeasts and filamentous fungi. In yeasts such as *Saccharomyces cerevisiae* and *Candida albicans*, highly branched *N*-linked mannans are bound to proteins and total more than 100 mannosyl residues per molecule. These mannans cover the surface of the cell wall and are not covalently bound to the polysaccharide core of the cell wall. In contrast, in *Aspergillus fumigatus*, which can serve of a model for ascomycetous molds, cell wall mannans (with an average of 80 mannose residues per chain) are integral parts of the cell wall since they are covalently bound to the glucan-chitin core (7). In addition, *Aspergillus* mannan contains galactofuranose residues and is released during fungal infection, making it an immunomodulatory molecule and a biomarker used to diagnose invasive aspergillosis (8–10). However, to date its biosynthesis had been unknown.

Pioneering studies in the model species *S. cerevisiae* have identified a series of mannosyltransferases which are sequentially involved in mannan biosynthesis. Addition of the first α 1,6 mannose to the N-glycan of the glycoprotein is catalyzed by Och1p. Extension of the α -1,6-mannan chain is due to the multienzymatic complexes mannan polymerase I (Pol I) and Pol II (11). Proteins of these complexes are encoded by *Mnn9*, *Van1*, *Anp1*, *Mnn10*, *Mnn11*, and *Hoc1* genes. Branching of the α -1,6-mannan backbone is initiated by *Mnn2* and *Mnn5* to produce short α -1,2-mannan oligosaccharides. This branched-core mannan is subsequently modified by phosphorylation by *Mnn6* and can be capped by α -1,3-mannose added by *Mnn1*. Even though the genes involved in mannan synthesis have been identified, the respective synthetic events in the biosynthetic organization of yeast mannans are not fully understood.

In filamentous fungi and especially in *Aspergillus fumigatus*, the model species in which the cell wall has been the most extensively studied, synthesis of the cell wall-bound mannan has not been elucidated. The mannan of *A. fumigatus* which is bound to the β -1,3-glucan-chitin core of the cell wall is a linear polymer with a repeating unit composed of four α -1,6- and α -1,2-linked mannoses with side chains of galactofuran (7, 12). The *in silico* search for putative yeast mannosyltransferases in *A. fumigatus* has identified 11 orthologous yeast α -1,6- and α -1,2-mannosyltransferases. Accordingly, the deletion of all 11 of the putative orthologs of the yeast mannosyltransferases responsible for establishing α -1,6- and α -1,2-mannose linkages was undertaken in *A. fumigatus* (13). However, even though the encoded *A. fumigatus* proteins had an active mannosyltransferase activity which was able to complement the yeast genes (13, 14), the successive deletion of these 11 mannosyltransferase genes did not affect the mannan content of the mycelial cell wall of *A. fumigatus*. The only phenotype of this mutant was a reduction of the mannan content of the conidial cell wall leading to a partial disorganization of the cell wall and defects in conidial dormancy without affecting the structural cell wall galactomannan (GM) of the mycelium. That study suggested that at least two sets of mannosyltransferases are responsible for the synthesis of cell wall mannans in the conidium and mycelium of *A. fumigatus*. Moreover, that study showed that genes with highly conserved sequence can code for proteins which have very different biological functions in yeasts and filamentous fungi. These considerations led us to investigate other orthologs of yeast mannosyltransferases with a function not associated with mannan polymerization in yeast. This is why we investigated the *KTR* genes, which were excluded from our initial study (13) for two reasons: (i) in yeast, these genes are exclusively involved in N- and O-glycan processing in yeast (15); (ii) the gene coding for one member of this family which contains three genes has been previously disrupted without any significant effect on the growth phenotype of the mutant (4). The data of this current study showed that in *A. fumigatus* the two members of the *KTR* family orthologous to the yeast *KTR4* and *KTR7* are mannosyltransferases responsible for the polymerization of the structural cell wall

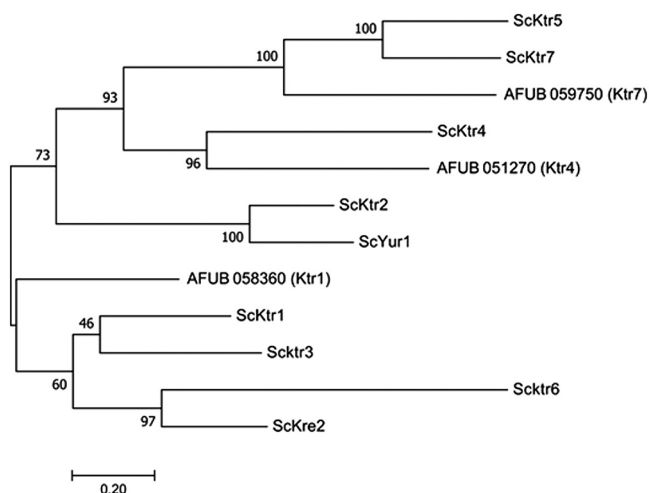


FIG 1 Phylogenetical tree of KTR genes in *A. fumigatus* and *S. cerevisiae*.

galactomannan. Their deletion led to a severe growth phenotype with a hyperbranched mycelium resulting from a lowered polarized growth, a strong defect in conidiation, a marked alteration of the conidial viability over time, and a reduction of virulence in mouse models.

(This work was presented in part at the Fungal Cell Wall 2017 Conference [Ensenada, Baja California, Mexico, 9 to 12 October 2017] and at the 4th Glycobiology World Congress (Rome, Italy, 17 to 18 September 2018).)

RESULTS

Phylogenetical analysis of Ktr proteins in *A. fumigatus* and construction of Δ Ktr mutant and revertant strains. The *A. fumigatus* KTR genes have very close sequence homologies with the *S. cerevisiae* KTR genes which belong to the GT15 family (www.Cazy.org). A phylogenetical analysis performed with the MUSCLE software with the 9 KTR members of *S. cerevisiae* showed that *A. fumigatus* UB_059750 (AFUA_5G12160) and AFUB_051270 (AFUA_5G02740) genes were closely related to ScKtr7 and ScKtr4, respectively (Fig. 1). The third member (AFUB_058360 [AFUA_5G10760]) was more distantly related to the yeast Ktr members (Fig. 1). In accordance with this phylogenetic tree, AFUB_058360, AFUB_051270, and AFUB_059750 were named KTR1, KTR4, and KTR7, respectively. These three proteins share 31% to 37% identity. Transcriptome sequencing (RNAseq) gene expression data from *A. fumigatus* have been recently published (16). All three KTR genes are expressed in resting conidia, germ tubes, and mycelia. In order to investigate the function of these KTR genes in *A. fumigatus*, deletion of *KTR1*, *KTR4*, and *KTR7* and construction of the complemented strains were carried out with the β -rec/six system as described earlier (17). The validation of mutant strains was done by Southern blot analysis as shown in Fig. S1 in the supplemental material.

Mycelial growth and morphology. Parental, Δ ktr, and complemented strains were grown in liquid and on agar minimum media (MM) and Sabouraud media. After 2 days at 37°C, the growth of Δ ktr4 and Δ ktr7 mutants was severely reduced in MM as well as on Sabouraud agar media (Fig. 2). The growth defect was more severe at 50°C, under which conditions almost no growth of Δ ktr4 and Δ ktr7 mutants was observed. In contrast, the Δ ktr1 mutant and Δ ktr4::KTR4 and Δ ktr7::KTR7 complemented strains showed normal growth comparable to that seen with the parental strain. The addition of 6% KCl or 1 M sorbitol to the medium as an osmostabilizer did not restore the parental growth phenotype (data not shown). A statistically significant reduction of growth of Δ ktr4 and Δ ktr7 mutants was also observed in liquid media (Fig. 3). After 18 to 22 h of culture in liquid media, parental and complemented strains produced long and thin hyphae (Fig. 4). In contrast, hyphae of Δ ktr4 and Δ ktr7 mutants were denser

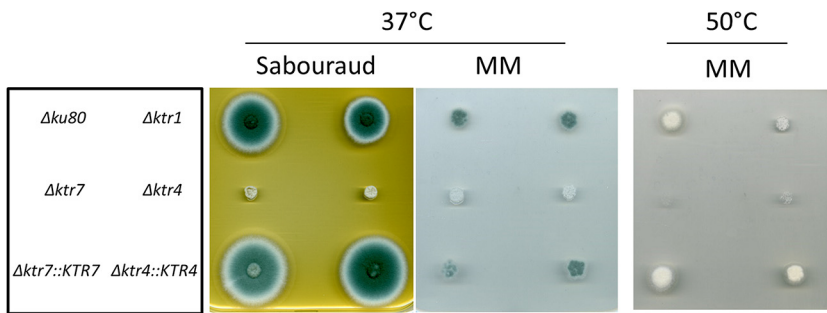


FIG 2 Growth of the parental $\Delta ku80$ strain, $\Delta ktr1$, $\Delta ktr4$ and $\Delta ktr7$ mutants, and $\Delta ktr4::KTR4$ and $\Delta ktr7::KTR7$ revertant strains on solid media. Strains were grown on either Sabouraud or minimum (MM) solid medium. A total of 10^3 conidia of each strain were spotted on media and incubated at 37°C or 50°C for 48 h.

and hyperbranched. Accordingly, $\Delta ktr4$ and $\Delta ktr7$ mutants produced numerous small mycelium balls in both versions of the liquid media (Fig. 3B).

Sensitivity to drugs. Both the $\Delta ktr4$ and $\Delta ktr7$ mutants were more sensitive to calcofluor white (CFW), Congo red, and SDS than the parental strain and the $\Delta ktr1$ mutant and their respective complemented strains (see Table S1 in the supplemental material). MICs of 7.5, 2.5, and 100 $\mu\text{g/ml}$ were estimated for calcofluor white, Congo red, and SDS, respectively, for both the $\Delta ktr4$ and $\Delta ktr7$ mutants versus MICs of 30 and 40 $\mu\text{g/ml}$ and 1 mg/ml, respectively, for the parental strain, suggesting an alteration of the cell wall organization or permeability. In contrast, no difference of growth was observed between the parental and all mutant strains in the presence of menadione, H_2O_2 , amphotericin B, caspofungin, posaconazole, or itraconazole (Table S1).

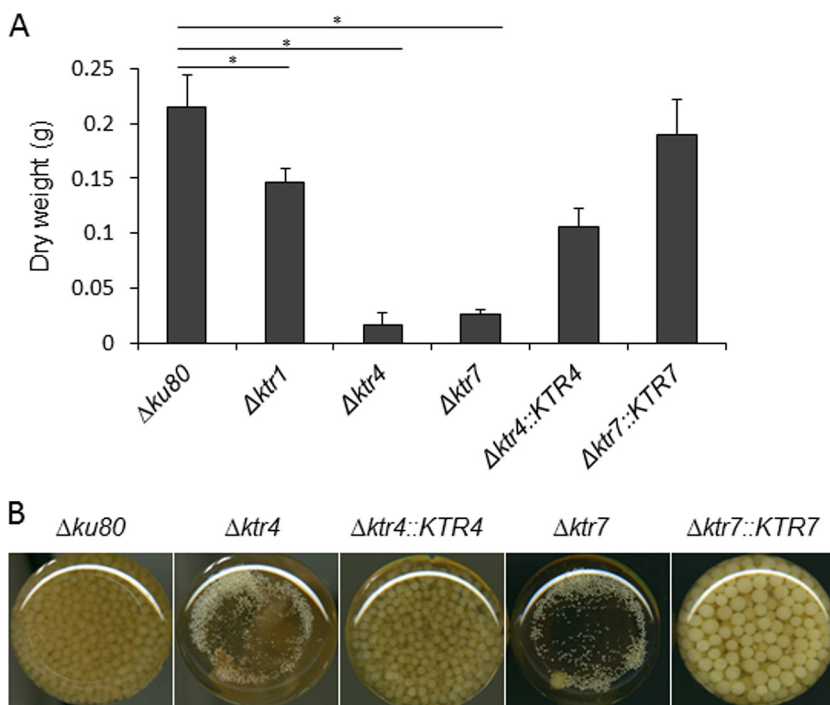


FIG 3 Growth of parental $\Delta ku80$ strain, $\Delta ktr1$, $\Delta ktr4$, and $\Delta ktr7$ mutants, and $\Delta ktr4::KTR4$ and $\Delta ktr7::KTR7$ revertant strains in liquid media. Strains were grown in Sabouraud liquid media. Flasks (50 ml) were inoculated with 10^6 conidia and incubated under shaking conditions (150 rpm/min) at 37°C for 24 h. (A) Mycelium biomass. The biomass/flask was quantified by the weight of the mycelium after drying at 80°C. Each value of mycelium dry weight represents the average of data from three independent replicates (*, $P < 0.05$; error bars represent standard deviations). (B) Gross morphology of mycelium.

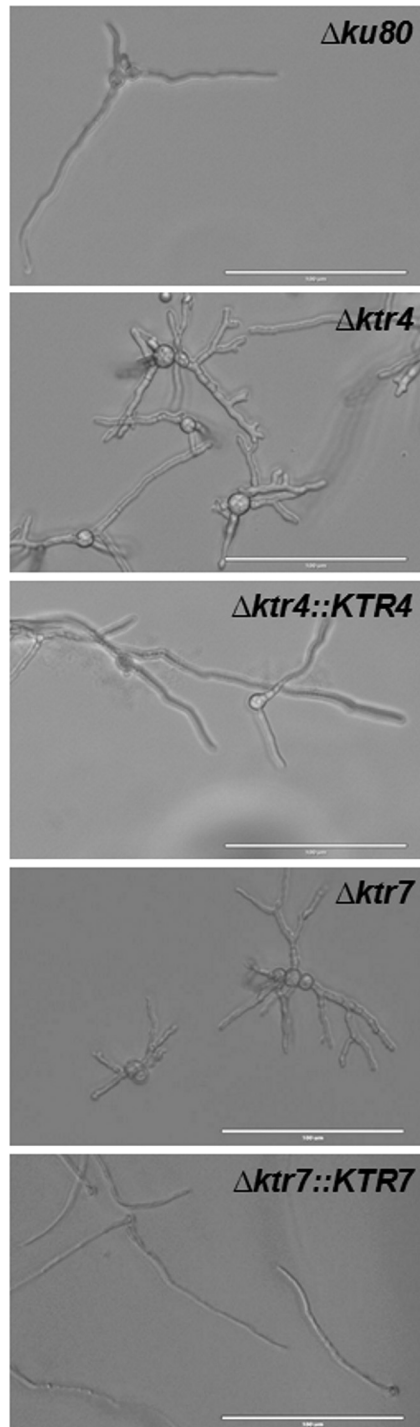


FIG 4 Morphology of germinated conidia of parental $\Delta ku80$ strain, $\Delta ktr4$ and $\Delta ktr7$ mutants, and $\Delta ktr4::KTR4$ and $\Delta ktr7::KTR7$ revertant strains after 20 ± 2 h of incubation in MM liquid medium at 37°C . White bars represent $100 \mu\text{m}$.

Conidiation, conidial morphology, conidium survival, and conidial germination. In comparison to the parental strain, the $\Delta ktr1$ mutant, and the $\Delta ktr4::KTR4$ and $\Delta ktr7::KTR7$ complemented strains, the $\Delta ktr4$ and $\Delta ktr7$ mutants produced very low amounts of conidia, representing 1.4% and 4.6% of the total amount of conidia produced by the parental strain in malt medium, respectively, and 4.4% and 10.2% in malt supplemented with 6% KCl, respectively (Table 1). The supplementation of the

TABLE 1 Conidiation of the Δktr mutants and the parental $\Delta ku80$ strains on malt agar in the presence or absence of 6% KCl^a

Strain	Growth condition	
	Malt	Malt-6% KCl
$\Delta ku80$	1,865 ± 688 × 10 ⁶	1,199 ± 205 × 10 ⁶
$\Delta ktr1$	2,663 ± 338 × 10 ⁶	ND
$\Delta ktr4$	26.8 ± 12.5 × 10 ⁶	55 ± 10 × 10 ⁶
$\Delta ktr7$	82.3 ± 24 × 10 ⁶	122 ± 33 × 10 ⁶
$\Delta ktr4::KTR4$	1,714 ± 305 × 10 ⁶	878 ± 123 × 10 ⁶
$\Delta ktr7::KTR7$	1,711 ± 475 × 10 ⁶	727 ± 89 × 10 ⁶

^aStrains were inoculated by spanning 50 μ l of suspensions of 10⁶ conidia/ml on slants of malt or malt-6% KCl solid media and were incubated at 37°C for 1 night and 2 weeks at room temperature. Produced conidia were collected with 0.05% Tween 20 solution and quantified. Values represent means ± standard deviations (SD) of results from three different experiments. ND, not determined.

medium with 6% KCl or 1 M sorbitol (data not shown) did not restore conidiation, showing that the strong conidiation defect of both the $\Delta ktr4$ and $\Delta ktr7$ mutants was not due to higher sensitivity to osmotic pressure of the mutants. The morphology of the conidia of the $\Delta ktr4$ and $\Delta ktr7$ mutants was altered. When they were produced on malt-KCl medium, conidia from the parental and complemented strains and the $\Delta ktr1$ mutant appeared as round spheres with an average diameter of 3 (± 0.4) μ m. Conidia produced by the $\Delta ktr4$ and $\Delta ktr7$ mutants were heterogeneous in size and larger than those produced by the parental strain, with average diameters of 3.4 μ m (± 0.9 μ m) and 4.05 μ m (± 1.5 μ m), respectively. In addition, the level of labeling of the $\Delta ktr4$ and $\Delta ktr7$ mutant conidia by CFW was much higher than that observed with the parental strain. Moreover, the levels of labeling of the conidia with fluorescein isothiocyanate (FITC) were also different. The conidia from parental and complemented strains were FITC labeled (at the cell wall) to only a slight extent, whereas 66% and 31% of $\Delta ktr4$ and $\Delta ktr7$ mutant conidia, respectively, were strongly intracellularly labeled (Fig. S2), suggesting that the deletion of *KTR4* and *KTR7* induced an increase of conidial permeability. This defect in cell wall permeability was associated with a reduction of conidia viability (Fig. S3). For example, conidia from the parental and complemented strains were resistant to storage in water at 4°C whereas 59% and 93% of $\Delta ktr4$ mutant conidia died after 1 and 2 months of storage under the same condition. Similar loss of viability was obtained for the $\Delta ktr7$ mutant (data not shown).

The $\Delta ktr4$ and $\Delta ktr7$ mutants germinated faster than their parental strain. On malt agar, conidia from parental, $\Delta ktr1$ mutant, and $\Delta ktr4::KTR4$ and $\Delta ktr7::KTR7$ complemented strains started to germinate after 4 h of incubation in the medium whereas 20% and 32% of $\Delta ktr4$ and $\Delta ktr7$ conidia, respectively, had already germinated by the same time (Fig. 5A). After 5 h, 50% of $\Delta ktr4$ and $\Delta ktr7$ conidia had germinated versus 24% of the conidia of the parental strain. Moreover, the pattern of germination of the $\Delta ktr4$ and $\Delta ktr7$ mutant strains was different from that seen with the parental strain. First, swollen conidia from $\Delta ktr4$ and $\Delta ktr7$ mutant strains were 1.7 times larger and more heterogeneous in size than those from parental strain (Fig. 5B). Second, the emergence of germ tubes was different in the parental and mutant strains. Germinating conidia of the parental strain produced successively first, second, and third germ tubes (see Movie S1 in the supplemental material). At 16 h, 51% and 41% of the parental conidia produced 2 and 3 germ tubes, respectively, with an average of 2.4 germ tubes/conidium (Fig. 5C). The second germ tube was issued at 180° from the first one; the third one at 90°. In contrast, the conidia of the $\Delta ktr4$ and $\Delta ktr7$ mutant strains produced up to 7 germ tubes, with averages of 3.7 and 3.9 germ tubes/conidium, respectively (Fig. 5C; see also Movie S2), and several germ tubes emerged simultaneously from swollen Δktr conidia without any specific location of the emergence site. Taken together, these data showed that the deletion of *KTR4* and *KTR7* affected growth polarization during germ tube emergence.

Protein glycosylation and cell wall analysis. Matrix-assisted laser desorption ionization–time of flight (MALDI-TOF) spectra of protein N-glycans were similar for the

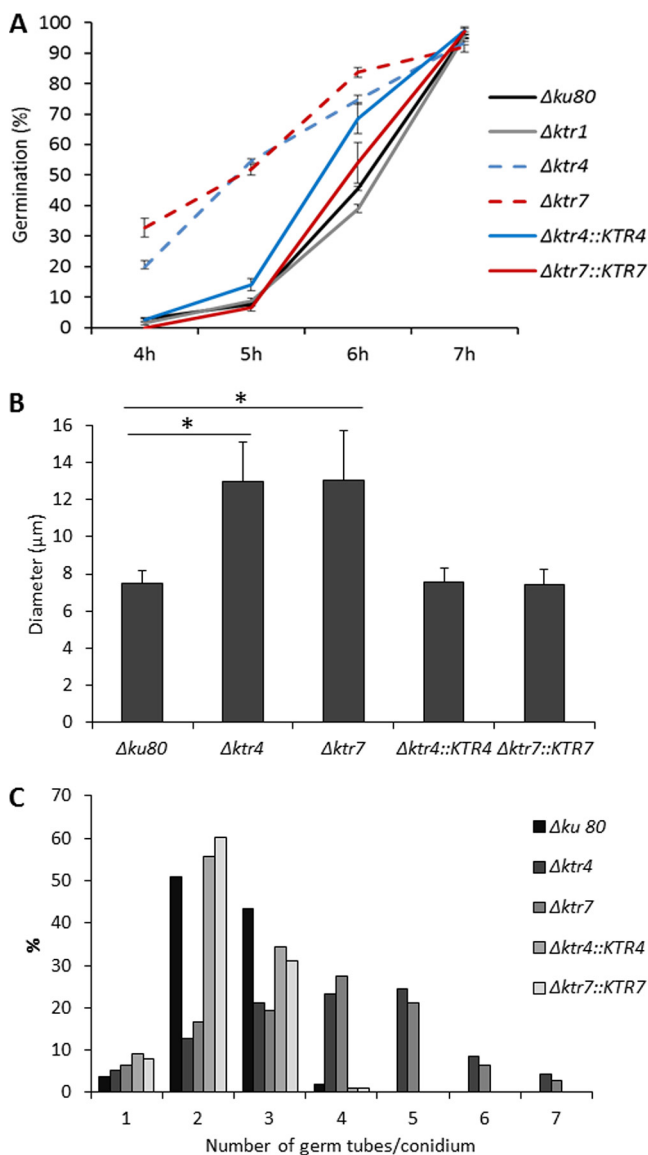


FIG 5 Conidial germination of parental $\Delta ku80$ strain, $\Delta ktr1$, $\Delta ktr4$, and $\Delta ktr7$ mutants, and $\Delta ktr4::KTR4$ and $\Delta ktr7::KTR7$ revertant strains. (A) Germination. Conidia ($5 \mu\text{l}$ of 2.10^6 conidia/ml suspension) were spotted on a slide of Sabouraud agar medium and incubated at 37°C under conditions of a humid atmosphere. Percentage of germination was quantified by bright-field counting of germinated and nongerminated conidia under a microscope. Each value represents the average of data from three independent replicates. Differences in the percentages of germination of $\Delta ktr4$ and $\Delta ktr7$ mutants were significant at 4, 5, and 6 h ($P < 0.0001$; error bars represent standard deviations). (B and C) The size of germinated conidia (B) and the number of germ tubes/conidium (C) were determined after 16 h of incubation in liquid MM medium at 37°C . Each value represents an average of data resulting from the counting of hundred conidia. (*, $P < 0.001$; error bars represent standard deviations).

parental and $\Delta ktr4$ and $\Delta ktr7$ mutant strains, with ion masses from m/z 1,419.55 to 2,391.91 at an increment of 162 (Fig. S4). These ion masses were in agreement with the presence of 2 GlcNAc and 6 to 12 hexose residues as previously described (18). These data indicated that the deletion of *KTR4* and *KTR7* did not induce a modification of the N-glycosylation of proteins. In contrast, the mannan content of the cell wall was affected by the deletion of *KTR4* and *KTR7*. The chemical composition of the alkali-insoluble (AI) and alkali-soluble (AS) fractions of the *A. fumigatus* cell wall of parental and mutant strains has been analyzed. No significant difference was observed in the monosaccharide content of the AS fraction of the $\Delta ktr4$ and $\Delta ktr7$ mutant strains in comparison to the parental and complemented strains (data not shown). On the other

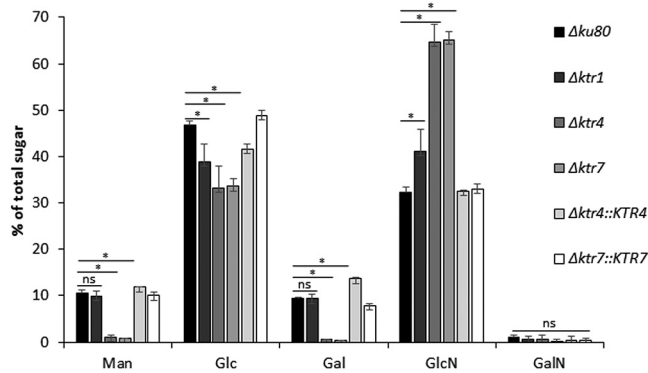


FIG 6 Monosaccharide composition of the alkali-insoluble fraction of the cell wall of the parental $\Delta ku80$ strain, $\Delta ktr1$, $\Delta ktr4$, and $\Delta ktr7$ mutants, and $\Delta ktr4::KTR4$ and $\Delta ktr7::KTR7$ revertant strains. The cell wall alkali-insoluble fraction (AI) was purified from mycelium grown for 24 h in liquid Sabouraud medium at 37°C (expressed as a percentage of total hexoses plus hexosamines). Monosaccharides were quantified after total acid hydrolysis and chromatography analysis. Each value represents an average of data from three independent triplicates. Statistical differences between parental and mutant strains are indicated as follows: ns, not significant; *, $p < 0.01$; error bars represent standard deviations. Man, mannose; Glc, glucose; Gal, galactose; GlcNAc, N-acetylglucosamine; GalNAc, N-acetylgalactosamine.

hand, an almost complete loss of the galactomannan content associated with a compensatory doubling of the chitin amount was observed in the AI fraction of the $\Delta ktr4$ and $\Delta ktr7$ mutants in comparison to the parental strain (Fig. 6). These data showed that deletion of *KTR4* and *KTR7* led to the loss of the cell wall galactomannan (GM) cross-linked to the glucan-chitin core and suggested that Ktr4p and Ktr7p were mannosyltransferases involved in the biosynthesis of the GM.

Mannosyltransferase activity of the recombinant protein Ktr4p. A Ktr4p recombinant (r-Ktr4) protein with a M_r of 43 kDa was produced in *Escherichia coli*. To test the putative mannosyltransferase activity, the r-Ktr4 protein was incubated with GDP-mannose as the substrate donor and α -1,2 mannobiose or α -1,6 mannobiose as the acceptor. Ktr4p was able to use both acceptors to produce a new product (Fig. 7). Gel filtration chromatography performed on a TSK-G-oligo-PW column and MALDI-TOF mass spectrometry have shown that the products obtained with an α -1,2 mannobiose or α -1,6 mannobiose acceptor were trisaccharides. The trisaccharide products were then characterized by exo- α -mannosidase digestion. For both acceptors, the reaction products were resistant to α -1,6-mannosidase treatment but were degraded by jack bean α -mannosidase and α -1,2-mannosidase treatments (Fig. 7), showing that the trisaccharide products contained a mannose at the nonreducing end linked through a α -1,2 linkage. These data showed that Ktr4p had α -1,2-mannosyltransferase activity and was able to use both α -1,2- and α -1,6-mannobiose as an acceptor to add one mannose residue.

Virulence. The virulence of the $\Delta ktr4$ mutant was tested in a mouse model of invasive aspergillosis using cyclophosphamide/cortisone acetate as an immunosuppressive treatment. The parental and complemented strains showed the same survival curves, with no mouse surviving 6 days after infection, whereas 30% of the mice remained alive in the cohort infected by the $\Delta ktr4$ mutant. Statistical analysis showed that the $\Delta ktr4$ mutant was significantly less virulent than the parental and complemented strains (Fig. S5). Histopathological analysis was performed 3 days postinfection. Multifocal inflammatory lesions, centered on bronchi/bronchioles and with secondary extension to alveoli, containing filamentous fungi were observed with both the parental and $\Delta ktr4$ strains (Fig. S6). However, the $\Delta ktr4$ mutant displayed reduced invasion of alveoli and large blood vessels in comparison to the parental strain.

DISCUSSION

This study and previous ones have shown that a high number of mannosyltransferases are functional in *A. fumigatus* (4, 13, 14, 19). A major impediment to under-

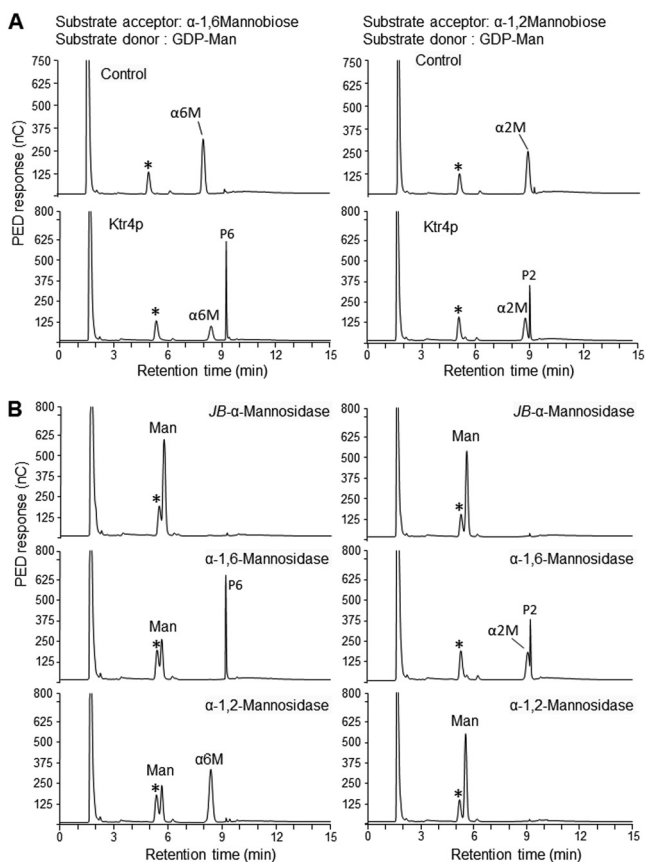


FIG 7 Ktr4p enzyme activity. (A) HPLC analysis of the products obtained after incubation of recombinant ktr4p with GDP-mannose and mannobiose (α -1,6-mannobiose or α -1,2-mannobiose). HPLC profiles were obtained after incubation of nontreated (Ktr4p) or heat-inactivated (Control) Ktr4p with mannobiose and GDP-mannose. (B) HPLC analysis of products submitted to exo- α -mannosidase digestions (PED, pulsed electrochemical detection; *JB*- α -Mannosidase, *Jack bean* α -mannosidase; α 2M, α -1,2-mannobiose; α 6M, α -1,6-mannobiose; Man, mannose; *, contaminant from buffer; P6, trisaccharide obtained in the presence of α -1,6-mannobiose; P2, trisaccharide obtained in the presence of α -1,2-mannobiose). *Jack bean* α -mannosidase fully degraded both acceptors (α 2M and α 6M) and products (P2 and P6) to release mannose residue, showing the α configuration of all mannose residues. α -1,6-Mannosidase degraded the α 6M but not the P6. α -1,2-Mannosidase degraded α 2M and P2 into mannose and P6 into α 6M and mannose.

standing the respective roles of all mannosyltransferases is their putative redundancy due to the lack of specificity of the different mannosyltransferases as seen at least *in vitro* in yeast, where mannosyltransferases can compensate for each other (7, 8). In *S. cerevisiae*, Ktr orthologs belong to the GT15 family in the CAZy database and have been characterized as α -1,2-mannosyltransferases playing a role in N- and O-mannosylation of glycoproteins (15, 20, 41, 53). Here, it was shown that although *A. fumigatus* ktr4p (Afktr4p) and Afktr7p share high sequence homologies with the yeast Ktrp orthologs and a mannosyltransferase activity, the deletion of *A. fumigatus* KTR4 and KTR7 genes did not alter protein mannosylation but led to the loss of the cell wall galactomannan. This report provides another clear example of the finding that orthologous genes code for proteins that may have very different biological functions in yeasts and filamentous fungi even though they have very related enzymatic activities, at least *in vitro*. It shows that the biosynthesis of the *A. fumigatus* mannans uses transferases and pathways different from those existing in yeasts. However, even in yeasts, the composition of the cell wall mannans, the number of genes involved in their synthesis, and the phenotype of the respective mutants differ from species to species. The elongation of the poly- α 1,6-mannan backbone in *S. cerevisiae* is carried out by the mannose Pol I (Man Pol I) and Pol II complexes to build up the α -1,6-mannan backbone (21–24). Mnn9 is a

member of these two complexes, but its quantitative contribution to α -1,6-mannan synthesis has not been clarified. In *C. albicans*, Mnn9 is the major contributor to the extension of the α -1,6-backbone since a deletion of *MNN9* resulted in the loss of 50% of the cell wall mannan. Another example can be found in the elongation of the α -1,2-mannan side chains. In *S. cerevisiae*, only 2 genes are responsible for the elongation of the α -1,2-mannan side chain whereas six paralogs of the Mnn2/Mnn5 genes were identified in *C. albicans* (54). We have previously shown that in *A. fumigatus*, genes orthologous to the yeast Man Pol I and II complexes are involved only in the synthesis of a specific amorphous alkali-soluble conidial mannan and are not involved in the synthesis of the main galactomannan constitutive of the cell wall of the mycelium and conidium (13, 14). This can be associated with the difference in the structures of long mannans in yeast and molds. In yeast, it is a branched structure directly anchored to proteins but not covalently bound to the cell wall structural polysaccharides, whereas in *A. fumigatus*, it is a repeat unit containing a linear structure covalently bound to the core polysaccharide.

KTR1 is the third *KTR* homolog in *A. fumigatus* and has been previously analyzed by Wagener et al. (4). Deletion of the *KTR1* gene was repeated in this study using the *akuB* $\Delta ku80$ CEA17 background, which was different from the wild-type strain D141 and its ΔkuA Afs35 derivative used previously by Wagener et al. (4) since different morphotypes from different genetic backgrounds can arise in *A. fumigatus*. The deletion of the *KTR1* in the *akuB* $\Delta ku80$ CEA17 mutant confirmed the results from the previous study (4) and showed that deletion of *KTR1* led to a very weak phenotype compared to those seen with the $\Delta ktr4$ and $\Delta ktr7$ mutants. Similar findings were obtained in *Beauveria bassiana*, where deletion of *KTR4* and *KRE2* induced drastic phenotypes and deletion of *KTR1* led only to a decrease in fungal thermotolerance (25). Such a lack of functional redundancy between members of the same gene family is common in filamentous fungi and especially in *A. fumigatus*. Even in cases in which similar enzymatic functions have been identified in the different members of a family, the phenotypes of the mutant lacking the encoding gene can be very different, ranging from the absence of the corresponding phenotype to a drastic or even lethal phenotype. This has been shown for the members of the Gel family and the Chs family in *A. fumigatus* (26–28).

The two major morphological phenotypes of the $\Delta ktr4$ and $\Delta ktr7$ mutants are the production of poorly viable conidia and a strong defect in vegetative growth. The deletion of *KTR4* and *KTR7* induced a loss of polarity during conidial germination and hyphal elongation. Establishment of the polarity in filamentous fungi is composed of three sequential steps. First, there is a deposition of cortical markers which establishes an axis of polarity and deposit. Next, products of key polarity genes such as the *CDC42/RAC1* module and polarisome components are recruited to the cortical markers. Finally, activity of the cell growth machinery involving actin and tubulin and leading to the sequential supply of proteins, lipids, and polysaccharides to the hyphal tip deposition of cell wall biosynthetic enzymes adds new cellular components in the correct place, resulting in asymmetric growth (29–32). In addition to mannan synthesis, polarization of germ tube growth requires also an appropriate deposition of two other structural components of the cell wall (β -1,3-glucan and chitin) (26, 33). In contrast, the absence of synthesis of α -glucan or β -1,3/1,4-glucan or galactosaminogalactan (GAG) did not alter the filamentous polarized growth (34–36), showing that only the three-dimensional (3D) structural skeleton of the cell wall chitin- β -1,3-glucan-GM plays an essential role in the establishment of polarity. Interestingly, the absence of cell wall GM was not compensated by the presence of the high amount of chitin seen in the cell wall of the $\Delta ktr4$ and $\Delta ktr7$ mutants to maintain normal filamentous growth. The data from the current study provide a great example of the need to have balanced accumulations of structural cell wall polysaccharides to avoid a loss of the dominance of the apical Spitzenkörper in growing hyphae and for the maintenance of the right polarity. However, the data from this study show also that the requirement of cell wall organization is less important in liquid medium than under aerobic conditions, under which the filamentous growth is more severely altered. Similarly, in our experimental murine

model of aspergillosis, the $\Delta ktr4$ mutant displayed reduced mycelium development which remained less pronounced than that seen in agar media (see Fig. S6 in the supplemental material), showing that the phenotype is highly dependent on growth conditions and explaining why the virulence defect was not so drastic as would be expected from the very altered *in vitro* phenotype.

This study showed that the GM cell wall biosynthesis pathway is independent of the protein mannosylation pathway and that *ktr4* and *ktr7* are key enzymes essential for the production of the constitutive cell wall galactomannan. Double deletion of *KTR4* and *KTR7* led to a phenotype similar to that seen with the single mutants (not shown), indicating that *ktr4p* and *ktr7p* are involved in the cell wall galactomannan biosynthetic pathway. The biosynthesis of galactomannan requires two different and separate pathways responsible for the synthesis of the galactofuran and the mannan elongation. First, the synthesis of the side chains of the GM is under the control of Golgi galactofuranosyltransferases, which use UDP galactofuranose as substrate (37, 38). However, the addition of galactofuranose is not a prerequisite either for the polymerization of mannan or for its incorporation in cell wall (39). Second, the mannan backbone assembly of galactomannan utilizes GDP-Man, which is transported at the Golgi level (40) and then used by Ktr proteins of *A. fumigatus*. These mannosyltransferases can accommodate either α -1,2-mannobiose or α -1,6-mannobiose as an acceptor. Since Ktr proteins in yeasts have been described previously as Golgi resident α -1,2-mannosyltransferases (4, 15, 41), these observations support a biosynthetic model according to which galactomannan is assembled in the Golgi apparatus and secreted to the plasma membrane before being cross-linked to cell wall β -glucan by extracellular transglycosidases. The chemical structure of the mannan chain (i.e., a tetra- α -1,2-mannoside repeat unit linked through an α -1,6 linkage) and its synthesis suggest specific forms of regulation of and/or cooperation between glycosyltransferases. Our current hypothesis is that *Ktr4p* and *Ktr7p* are α -1,2-mannosyltransferases acting sequentially during the synthesis of the tetra- α -1,2-mannoside unit. Examples of sequential addition of mannose residue have been described in yeast. *Mnn2* and *Mnn5* add the first and second branched α -1,2-mannose residues, respectively, on the α -1,6-mannan in yeast (42). The *Bmt3* and *Bmt1* β -1,2-mannosyltransferases add the first and second β -1,2-mannose residues, respectively, on N-mannan in *C. albicans* (43). These examples clearly show that the product of the first transferase activity is the acceptor of the second one and that the recognition of the acceptor by the transferase activity represents a critical point to drive the sequential addition of mannose residue. Such sequential activities could explain why both the *KTR4* and the *KTR7* genes are essential to the GM synthesis but are not redundant. The synthesis of the GM may also require the involvement of other α -1,2 and/or α -1,6-mannosyltransferase activities that remain to be identified to decipher the GM synthesis in *A. fumigatus*.

A recent study suggested that the DFG (for defective in filamentous growth) orthologs of the yeast *DFG5/DCW1* are required for the cross-linking between GM and β -glucan (L. Muszkiet, T. Fontaine, R. Beau, I. Mouyna, M. S. Vogt, J. Trow, B. P. Cormack, L.-O. Essen, G. Jouvion, and J.-P. Latgé, submitted for publication). Interestingly, deletions of orthologous DFG genes in *A. fumigatus* led to phenotypes closely related to those seen with the $\Delta ktr4$ and $\Delta ktr7$ mutants, showing the importance of the cross-linked GM in the cell wall. The search for new transglycosidases or regulators and protein chaperones involved in the synthesis of the mannan chain is currently under way.

MATERIALS AND METHODS

Growth conditions. The *A. fumigatus* parental strain used in this study was strain *akuB $\Delta ku80$ pyrG⁺* (44). Conidia were produced on 2% malt agar slants after 2 weeks of growth at room temperature and were recovered by vortex mixing with 0.05% (vol/vol) Tween 20 aqueous solution. The fungus was grown on agar (2%) or in liquid culture media as follows: *Aspergillus* minimum medium (MM) (45), Sabouraud (2% glucose, 1% mycopeptone) (Difco), or 2% malt (Cristomalt). For production of conidia, mutant strains were grown on malt agar medium supplemented with 6% KCl.

Phylogenetic analysis. Sequences of Ktr proteins were downloaded from the PubMed website and used for generating the alignment using MUSCLE v3.8.31 software (www.ebi.ac.uk/Tools/msa/muscle/). The software trimAl v3 was used to trim the alignments generated by MUSCLE, with the options `-gt 0.9` (for the fraction of sequences with a gap allowed) and `-cons 60` (for the minimum percentage of the positions in the original alignment to conserve). ProTest v2.4 software was used to select the best protein substitution model, namely, LG+I+G+F. Finally, maximum likelihood analyses were conducted with PHYML v3.0.1 to reconstruct phylogenetic trees. Support for the branches was determined from bootstrap analysis of 100 resampled data sets.

Nucleic acid manipulation. Genomic DNA was extracted as previously described (46). For Southern blot analysis, 10 μg of digested genomic DNA was subjected to size fractionation on 0.7% agarose and was blotted onto a positively charged nylon membrane (Hybond-N +; Amersham). For DNA extraction, mycelium was grown for 16 h at 37°C in Sabouraud liquid medium. For transformation experiments, MM was used. MM was supplemented with 150 $\mu\text{g}/\text{ml}$ hygromycin (Sigma) to isolate transformants. Cells of the *E. coli* T7 Shuffle strain, used for recombinant protein expression analysis, were grown on Luria-Bertani medium (47).

Construction of the Δktr deletion and revertant strains. A single-deletion mutant was constructed in the CEA17_ $\Delta\text{akuB}^{\text{KU80}}$ background (44) using the $\beta\text{-rec}/\text{six}$ site-specific recombination system (17). The self-excising $\beta\text{-rec}/\text{six}$ blaster cassette containing the hygromycin resistance marker was released from plasmid pSK529 via the use of an FspI restriction enzyme. Using GeneArt seamless cloning and assembly (Life Technologies, Carlsbad, CA, USA), the *KTR* replacement cassettes containing the marker module flanked by 5' and 3' homologous regions of the target gene generated by PCR (see Table S2 in the supplemental material) were cloned into the pUC19 vector. The corresponding replacement cassettes were released from the resulting vector via the use of FspI. The CEA17_ $\Delta\text{akuB}^{\text{KU80}}$ parental strain was transformed with the *KTR* replacement cassettes by electroporation to generate the single-deletion mutant. The transformants obtained were analyzed by diagnostic PCR and Southern blotting using the digoxigenin (DIG) probe protocol (Roche Diagnostics) (see Fig. S1 in the supplemental material). For the construction of the revertant strain, the mutant strain was cultivated in minimal medium without dextrose and with 2% xylose, which induces the excision of the selectable marker by recombination of the six recognition regions. The excision of the marker was verified by the absence of growth on malt medium containing the selectable marker. This excised strain was transformed with the *KTR* complementation cassette following the same protocol of transformation and control. All the primers used in this work are listed in Table S2.

Growth of the Δktr mutants. The mycelial growth was assessed in MM and Sabouraud agar media after spotting 10^3 conidia (5 μl) of each strain. Petri dishes were incubated for 48 h at 37°C and 50°C. Growth was also monitored in Sabouraud liquid media as follows: 150-ml flasks with 50 ml of media were inoculated with 10^6 conidia and incubated with shaking (150 rpm/min) at 37°C for 24 h, and the mycelial dry weight was estimated after drying at 80°C until a constant weight was reached.

Conidiation and conidial morphology. Conidia (3 weeks old) were recovered from malt agar slants by the use of 0.05% Tween 20 aqueous solution. Conidial suspensions were filtered on a 40- μm -pore-size sterile cell strainer (Fisher Scientific), and conidia were counted using a Luna dual-fluorescence cell counter (Mokasience SARL). Permeability of the conidia with respect to FITC was investigated by incubating 200 μl of an aqueous suspension of conidia ($2 \cdot 10^7$ conidia/ml) with 30 μl of FITC solution (1 mg/ml in 0.1 M Na_2CO_3 , pH 9) during 3 h at room temperature in darkness. The conidia were washed three times with 0.05% Tween 20 solution before being subjected to observation under a fluorescence microscope (EvoSfl Life Technologies; excitation wavelength [λ_{exc}], 470/22 nm; emission wavelength [λ_{em}], 510/44 nm). For calcofluor white (CFW) staining, the conidial suspension was incubated with CFW solution (0.5 $\mu\text{g}/\text{ml}$) for 30 min at room temperature and observed with fluorescence microscopy (EvoS FL Life Technologies; λ_{exc} , 357/44 nm; λ_{em} , 447/60 nm).

To investigate conidial survival, conidia were kept in a Tween 20 (0.05%) aqueous solution at 4°C for up to 2 months and survival over time was estimated by CFU quantification on malt agar plates. Conidial germination was followed on Sabouraud agar medium for up to 7 h at 37°C. To follow the kinetics of germination, conidia were inoculated (final suspension, $5 \times 10^5/\text{ml}$) in 8-well plates (IBIDI) in liquid MM buffered with 165 mM MOPS (morpholinepropanesulfonic acid; pH 7) at 37°C. Films were recorded under a Nikon light microscope (magnification, $\times 40$; 1 photo/4 min) and analyzed by the use of ICY software (Institut Pasteur, France). The size of conidia was estimated under a microscope using logiciel Image J software (National Institutes of Health, USA).

Susceptibility of the Δktr mutant strains to antifungal compounds. To investigate the susceptibility of mutant and parental strains to antifungal compounds, 5×10^3 conidia were spotted on MM plates containing serial dilutions of the following compounds: CFW (2 to 30 $\mu\text{g}/\text{ml}$), Congo red (2.5 to 40 $\mu\text{g}/\text{ml}$), H_2O_2 (0.3 to 5 mM), and SDS (0.001% to 0.1%). Sensitivity to menadione (0.015 to 160 μM) was tested in liquid MM with resazurin method as previously described (48). Susceptibility to antifungal drugs was estimated by the Etest strips according to manufacturer recommendations (Bio-Merieux). Plates were incubated for 18 h at 37°C in a humid atmosphere. The MIC was determined as the lowest drug concentration at which the border of the elliptical inhibition zone intercepted the scale on the antifungal strip.

Pathogenicity of the Δktr4 mutant. For virulence assays in the mouse model of invasive aspergillosis, immunosuppression of mice was induced with 150 mg/kg of body weight of cyclophosphamide (Pras-Farma, Barcelona, Spain) administered intraperitoneally (i.p.) and 112 mg/kg of cortisone 21-acetate (Sigma; catalog no. C-3130) administered subcutaneously, on both day -3 and day -1 . Afterward, only cyclophosphamide (150 mg/kg) was used every 3 days until completion of the experiment. The body

weight of each mouse was recorded weekly in order to adjust the immunosuppression dosage. Conidial inocula were prepared by growing the strains on malt–6% KCl agar slants. Conidia were harvested using saline solution containing 0.01% Tween 20 (Sigma), washed, filtered through a 40- μ m-pore-size nylon sterile filter (to avoid clumping of conidia), and then counted in a hemacytometer chamber, and the concentration was then adjusted to 5×10^6 conidia/ml. On day 0, the animals were anaesthetized intramuscularly with 0.1 ml of a mixture of ketamine (Ketolar; Pfizer) (50 mg/ml) and xilacina clorhidrato (Rompum; Bayer) (2%) at final concentrations of 12.5 and 2 mg/ml, respectively, and then intranasally inoculated with 30 μ l of saline solution containing a total inoculum of 1.5×10^5 conidia per mice. The rates of survival of mice were plotted against time, and *P* values were calculated using the log rank (Mantel-Cox) test and GraphPad Prism 5. A *P* value of <0.05 was considered significant. Additionally, lungs removed from mice at 3 days postinfection were fixed in 10% neutral buffered formalin and embedded in paraffin, and 4-micron-thick serial sections were cut and stained with hematoxylin and eosin (HE) (to enable descriptions of histopathological lesions) and Grocott's methenamine silver (to detect fungi).

Carbohydrate analysis of the cell wall and culture supernatant. After 24 h of growth of the mycelium in Sabouraud liquid medium at 37°C with shaking at 150 rpm, mycelia and culture supernatants were separated by filtration. Cell wall fractions (alkali-soluble and alkali-insoluble fractions) were obtained after mycelium disruption and centrifugation as previously described (26). Polysaccharides from the cell wall were separated with respect to the function of their alkali solubility (26). Neutral hexoses were estimated by the phenol sulfuric method using glucose as the standard (49). Glucosamines (Osamines) were quantified by high-performance liquid chromatography (HPLC) after acid hydrolysis with 6 N HCl at 100°C for 6 h (50). Monosaccharides were identified and quantified by gas-liquid chromatography (GLC) after acid hydrolysis with 4 N trifluoroacetic acid at 100°C for 4 h (26).

N-Glycosylation of secreted proteins was investigated according to a previously described protocol (51). Briefly, 1 mg of protein was subjected to denaturation in 0.6 M Tris-HCl–6 M guanidium chloride for 1 h at 50°C, reduced with 20 mM dithiothreitol (DTT) for 4 h at 100°C, and finally alkylated with 110 mM iodoacetamide overnight at room temperature. After dialysis against water and freeze-drying, samples were digested with trypsin and then with PNGase F to release N-glycans. N-glycans were purified by solid-phase extraction using a C₁₈-SepPak column (Waters) and paper chromatography (Whatmann no. 3) and then analyzed by MALDI-TOF.

Matrix-assisted desorption ionization-time of flight (MALDI-TOF) mass spectrometry. MALDI-TOF mass spectra were acquired on an UltrafleXtreme mass spectrometer (Bruker Daltonics, Bremen, Germany). Mass spectra were acquired in positive reflectron mode using FlexControl software. Mass spectra were externally calibrated in the *m/z* range of 700 to 3,500 Da with a peptide standard mixture (Bruker-Daltonics, Germany) and with a malto-oligosaccharide mixture. Data were analyzed with Flex-analysis software (Bruker). Samples were prepared by mixing 2 μ l of an oligosaccharide solution–water (0.01 to 2 nmol)–2 μ l 2 mg/ml NaCl solution with 4 μ l of 2,5-dihydroxybenzoic acid matrix solution (10 mg/ml in CH₃OH/H₂O, 50:50 [vol/vol]). The samples (1 μ l) were spotted on the target (MTP target; Bruker) and dried at room temperature.

Production and enzymatic assay of recombinant Ktr4 protein. The DNA sequence of *KTR4* was synthesized by the use of Geneart gene synthesis (Thermo Fisher Scientific) using an *E. coli* codon table optimized by the manufacturer. Furthermore, the N-terminal sequence (amino acids [aa] 1 to 28), predicted as a signal peptide cleavage site by SignalP software, was removed. The construct was cloned in the pET28a(+) expression vector using N-terminal His tagging, and the *E. coli* T7 Shuffle strain (New England Biolabs) was used for the protein production. The production of recombinant protein was undertaken after IPTG (isopropyl- β -D-thiogalactopyranoside) induction as follows. A 400-ml volume of LB containing kanamycin (30 μ g/ml) was inoculated at an optimal density of 0.05 and shaken at 20°C and 150 rpm. When an optical density at 600 nm (OD₆₀₀) of 0.6 was reached, induction was performed by the addition of 1 mM IPTG for 18 h. After centrifugation (3,300 \times g, 10 min), the bacterial pellet was lysed with 8 mg of lysozyme–40 ml of 50 mM Tris-HCl buffer (pH 8) for 40 min at room temperature. The supernatant containing the tagged protein was purified using nickel-nitrilotriacetic acid (Ni-NTA) agarose beads (Life Technologies) according to the manufacturer's instructions. The protein was eluted with 250 mM imidazole, concentrated, and desalted using Amicon cells with a 10-kDa molecular weight cutoff (MWCO) (Merck Millipore). Determination of protein concentration was performed by the bicinchoninic acid (BCA) method, and 12% SDS-PAGE was used to verify protein purity. In spite of many attempts, it was impossible to produce a soluble recombinant form of the Ktr7 protein in *E. coli*, since it was exclusively found in inclusion bodies.

The mannosyltransferase activity assay was performed as previously described (52) with modifications. Briefly, 25 μ g of recombinant protein was incubated in 28 μ l of buffer (50 mM Tris, 75 mM KCl, 5% glycerol, 5 mM MnCl₂, 5 mM MgCl₂ [pH 7.5], 2 mM DTT) containing 6.7 mM GDP-Man (Sigma G5131) and 11 mM 6 α -mannobiose (Dextra M206) or 2 α -mannobiose (Sigma M1050) at 30°C overnight. To investigate glycoside linkages, reaction products were digested by the use of either jack bean exo- α -mannosidase (Sigma) (2.5 μ l of an enzymatic reaction mixture with 1.36 U enzyme activity and 10 μ l of 50 mM [pH 6.8] Na acetate buffer) or recombinant α -1,6-mannosidase (Biolabs) (2.5 μ l of enzymatic reaction mixture, 80 U of α -1,6-mannosidase, 20 μ l of 1 \times Biolabs buffer) or α -1,2-mannosidase (Prozyme) (2.5 μ l of enzymatic reaction with 0.2 mU of α -1,2-mannosidase–20 μ l of 1 \times Prozyme buffer). Mixtures were incubated for 18 h at 30°C. Digestion products were analyzed by high-pH anion-exchange chromatography (HPAEC) using a CarboPAC PA-1 column (Thermo Scientific, Villebon sur Yvette, France) (4.6 by 250 mm) and a pulsed electrochemical detector with the following gradient: an isocratic step of

98% eluent A (50 mM NaOH) and 2% eluent B (500 mM AcONa–50 mM NaOH) for 2 min, 2 to 15 min of a linear gradient (98% A/2% B to 65% A/35% B), 15 to 35 min of a linear gradient (65% A/35% B to 30% A/70% B), 35 to 37 min of a linear gradient (30% A/70% B to 0% A/100% B), 37 to 40 min under isocratic conditions with 100% B. The column was stabilized for 20 min under the initial conditions before injection was performed. Enzymatic products were purified by gel filtration chromatography on a TSK-Gel G-oligo-PW column (Tosoh Bioscience, Stuttgart, Germany) (7.8 by 300 mm) eluted with water at 0.5 ml/min. The column was calibrated with a mixture of malto-oligosaccharides. The M_w of the products was also analyzed by MALDI-TOF.

Ethics statement. All animal experiments performed at the Mycology Reference Laboratory were ethically approved by the Animal Welfare Committee of Instituto de Salud Carlos III and performed under the approved project license PROEX 324/16.

Statistical analysis. At least three biological replicates were performed per experiment; the statistical significance of the results was evaluated by a one-way variance analysis using JMP1 software (SAS Institute, Cary, NC, USA).

SUPPLEMENTAL MATERIAL

Supplemental material for this article may be found at <https://doi.org/10.1128/mBio.02647-18>.

FIG S1, PDF file, 0.2 MB.

FIG S2, PDF file, 0.9 MB.

FIG S3, PDF file, 0.05 MB.

FIG S4, PDF file, 0.1 MB.

FIG S5, PDF file, 0.04 MB.

FIG S6, PDF file, 0.4 MB.

TABLE S1, DOCX file, 0.03 MB.

TABLE S2, DOCX file, 0.03 MB.

MOVIE S1, MOV file, 2.5 MB.

MOVIE S2, MOV file, 2.7 MB.

ACKNOWLEDGMENTS

This research was funded by l'Agence Nationale pour la Recherche (Afulnf ANR-16-CE92-0039), la Fondation pour la Recherche Médicale (DEQ20150331722 LATGE Equipe FRM 2015), the French Government's Investissement d'Avenir program, and Laboratoire d'Excellence "Integrative Biology of Emerging Infectious Diseases" (grant ANR-10-LABX-62-IBEID).

REFERENCES

- Goto M. 2007. Protein O-glycosylation in fungi: diverse structures and multiple functions. *Biosci Biotechnol Biochem* 71:1415–1427. <https://doi.org/10.1271/bbb.70080>.
- Deshpande N, Wilkins MR, Packer N, Nevalainen H. 2008. Protein glycosylation pathways in filamentous fungi. *Glycobiology* 18:626–637. <https://doi.org/10.1093/glycob/cwn044>.
- Mouyna I, Kniemeyer O, Jank T, Loussert C, Mellado E, Aïmanianda V, Beauvais A, Wartenberg D, Sarfati J, Bayry J, Prévost M-C, Brakhage AA, Strahl S, Huerre M, Latgé J-P. 2010. Members of protein O-mannosyltransferase family in *Aspergillus fumigatus* differentially affect growth, morphogenesis and viability. *Mol Microbiol* 76:1205–1221. <https://doi.org/10.1111/j.1365-2958.2010.07164.x>.
- Wagener J, Echtenacher B, Rohde M, Kotz A, Krappmann S, Heesemann J, Ebel F. 2008. The putative α -1,2-mannosyltransferase AfMnt1 of the opportunistic fungal pathogen *Aspergillus fumigatus* is required for cell wall stability and full virulence. *Eukaryot Cell* 7:1661–1673. <https://doi.org/10.1128/EC.00221-08>.
- Hall RA, Bates S, Lenardon MD, MacCallum DM, Wagener J, Lowman DW, Kruppa MD, Williams DL, Odds FC, Brown AJP, Gow NAR. 2013. The Mnn2 mannosyltransferase family modulates mannoprotein fibril length, immune recognition and virulence of *Candida albicans*. *PLoS Pathog* 9:e1003276. <https://doi.org/10.1371/journal.ppat.1003276>.
- Goto M, Harada Y, Oka T, Matsumoto S, Takegawa K, Furukawa K. 2009. Protein O-mannosyltransferases B and C support hyphal development and differentiation in *Aspergillus nidulans*. *Eukaryot Cell* 8:1465–1474. <https://doi.org/10.1128/EC.00371-08>.
- Fontaine T, Simenel C, Dubreucq G, Adam O, Delepierre M, Lemoine J, Vorgias CE, Diaquin M, Latgé JP. 2000. Molecular organization of the alkali-insoluble fraction of *Aspergillus fumigatus* cell wall. *J Biol Chem* 275:27594–27607. <https://doi.org/10.1074/jbc.M909975199>.
- Lamoth F. 2016. Galactomannan and 1,3- β -D-glucan testing for the diagnosis of invasive aspergillosis. *J Fungi (Basel)* 2:22. <https://doi.org/10.3390/jof2030022>.
- Chai LYA, Vonk AG, Kullberg BJ, Verweij PE, Verschueren I, van der Meer JWM, Joosten LAB, Latgé J-P, Netea MG. 2011. *Aspergillus fumigatus* cell wall components differentially modulate host TLR2 and TLR4 responses. *Microbes Infect* 13:151–159. <https://doi.org/10.1016/j.micinf.2010.10.005>.
- Bozza S, Clavaud C, Giovannini G, Fontaine T, Beauvais A, Sarfati J, D'Angelo C, Perruccio K, Bonifazi P, Zagarella S, Moretti S, Bistoni F, Latgé J-P, Romani L. 2009. Immune sensing of *Aspergillus fumigatus* proteins, glycolipids, and polysaccharides and the impact on Th immunity and vaccination. *J Immunol* 183:2407–2414. <https://doi.org/10.4049/jimmunol.0900961>.
- Munro S. 2001. What can yeast tell us about N-linked glycosylation in the Golgi apparatus. *FEBS Lett* 498:223–227.
- Latgé JP, Kobayashi H, Debeaupuis JP, Diaquin M, Sarfati J, Wieruszkeski JM, Parra E, Bouchara JP, Fournet B. 1994. Chemical and immunological characterization of the extracellular galactomannan of *Aspergillus fumigatus*. *Infect Immun* 62:5424–5433.
- Henry C, Fontaine T, Heddergott C, Robinet P, Aïmanianda V, Beau R, Beauvais A, Mouyna I, Prevost M-C, Fekkar A, Zhao Y, Perlin D, Latgé J-P. 2016. Biosynthesis of cell wall mannan in the conidium and the mycelium of *Aspergillus fumigatus*. *Cell Microbiol* 18:1881–1891. <https://doi.org/10.1111/cmi.12665>.
- Lambou K, Perkhofer S, Fontaine T, Latgé J-P. 2010. Comparative func-

- tional analysis of the OCH1 mannosyltransferase families in *Aspergillus fumigatus* and *Saccharomyces cerevisiae*. *Yeast* 27:625–636. <https://doi.org/10.1002/yea.1798>.
15. Lussier M, Sdicu A-M, Bussereau F, Jacquet M, Bussey H. 1997. The Ktr1p, Ktr3p, and Kre2p/Mnt1p mannosyltransferases participate in the elaboration of yeast O- and N-linked carbohydrate chains. *J Biol Chem* 272:15527–15531.
 16. Mouyna I, Aïmanianda V, Hartl L, Prevost M-C, Sismeiro O, Dillies M-A, Jagla B, Legendre R, Coppee J-Y, Latgé J-P. 2016. GH16 and GH81 family β -(1,3)-glucanases in *Aspergillus fumigatus* are essential for conidial cell wall morphogenesis. *Cell Microbiol* 18:1285–1293. <https://doi.org/10.1111/cmi.12630>.
 17. Hartmann T, Dümig M, Jaber BM, Szewczyk E, Olbermann P, Morschhäuser J, Krappmann S. 2010. Validation of a self-excising marker in the human pathogen *Aspergillus fumigatus* by employing the beta-rec/six site-specific recombination system. *Appl Environ Microbiol* 76:6313–6317. <https://doi.org/10.1128/AEM.00882-10>.
 18. Morelle W, Bernard M, Debeauvais J-P, Buitrago M, Tabouret M, Latgé J-P. 2005. Galactomannoproteins of *Aspergillus fumigatus*. *Eukaryot Cell* 4:1308–1316. <https://doi.org/10.1128/EC.4.7.1308-1316.2005>.
 19. Krüger AT, Engel J, Buettner FFR, Routier FH. 2016. *Aspergillus fumigatus* Cap59-like protein A is involved in α 1,3-mannosylation of GPI-anchors. *Glycobiology* 26:30–38. <https://doi.org/10.1093/glycob/cwv078>.
 20. Reason AJ, Dell A, Romero PA, Herscovics A. 1991. Specificity of the mannosyltransferase which initiates outer chain formation in *Saccharomyces cerevisiae*. *Glycobiology* 1:387–391.
 21. Rodionov D, Romero PA, Berghuis AM, Herscovics A. 2009. Expression and purification of recombinant M-Pol I from *Saccharomyces cerevisiae* with α -1,6 mannosyltransferase activity. *Protein Expr Purif* 66:1–6. <https://doi.org/10.1016/j.pep.2009.02.013>.
 22. Jungmann J, Munro S. 1998. Multi-protein complexes in the cis Golgi of *Saccharomyces cerevisiae* with alpha-1,6-mannosyltransferase activity. *EMBO J* 17:423–434. <https://doi.org/10.1093/emboj/17.2.423>.
 23. Jungmann J, Rayner JC, Munro S. 1999. The *Saccharomyces cerevisiae* protein Mnn10p/Bed1p is a subunit of a Golgi mannosyltransferase complex. *J Biol Chem* 274:6579–6585.
 24. Stolz J, Munro S. 2002. The components of the *Saccharomyces cerevisiae* mannosyltransferase complex M-Pol I have distinct functions in mannan synthesis. *J Biol Chem* 277:44801–44808. <https://doi.org/10.1074/jbc.M208023200>.
 25. Wang J-J, Qiu L, Cai Q, Ying S-H, Feng M-G. 2014. Three α -1,2-mannosyltransferases contribute differentially to conidiation, cell wall integrity, multistress tolerance and virulence of *Beauveria bassiana*. *Fungal Genet Biol* 70:1–10. <https://doi.org/10.1016/j.fgb.2014.06.010>.
 26. Muszkieta L, Aïmanianda V, Mellado E, Gribaldo S, Alcázar-Fuoli L, Szewczyk E, Prevost M-C, Latgé J-P. 2014. Deciphering the role of the chitin synthase families 1 and 2 in the *in vivo* and *in vitro* growth of *Aspergillus fumigatus* by multiple gene targeting deletion. *Cell Microbiol* 16:1784–1805. <https://doi.org/10.1111/cmi.12326>.
 27. Mouyna I, Fontaine T, Vai M, Monod M, Fonzi WA, Diaquin M, Popolo L, Hartland RP, Latgé JP. 2000. Glycosylphosphatidylinositol-anchored glucanase transferases play an active role in the biosynthesis of the fungal cell wall. *J Biol Chem* 275:14882–14889.
 28. Gastebois A, Fontaine T, Latgé J-P, Mouyna I. 2010. β -(1-3)Glucanase transferase Gel4p is essential for *Aspergillus fumigatus*. *Eukaryot Cell* 9:1294–1298. <https://doi.org/10.1128/EC.00107-10>.
 29. Takeshita N. 2016. Coordinated process of polarized growth in filamentous fungi. *Biosci Biotechnol Biochem* 80:1693–1699. <https://doi.org/10.1080/09168451.2016.1179092>.
 30. Riquelme M, Aguirre J, Bartnicki-García S, Braus GH, Feldbrügge M, Fleig U, Hansberg W, Herrera-Estrella A, Kämper J, Kück U, Mourino-Pérez RR, Takeshita N, Fischer R. 2018. Fungal morphogenesis, from the polarized growth of hyphae to complex reproduction and infection structures. *Microbiol Mol Biol Rev* 82:e00068-17. <https://doi.org/10.1128/MMBR.00068-17>.
 31. Harris SD, Momany M. 2004. Polarity in filamentous fungi: moving beyond the yeast paradigm. *Fungal Genet Biol* 41:391–400. <https://doi.org/10.1016/j.fgb.2003.11.007>.
 32. Oda K, Bignell E, Kang SE, Momany M. 2017. Transcript levels of the *Aspergillus fumigatus* Cdc42 module, polarisome, and septin genes show little change from dormancy to polarity establishment. *Med Mycol* 55:445–452. <https://doi.org/10.1093/mmy/myw085>.
 33. Dichtl K, Samantaray S, Aïmanianda V, Zhu Z, Prevost M-C, Latgé J-P, Ebel F, Wägener J. 2015. *Aspergillus fumigatus* devoid of cell wall β -1,3-galactan is viable, massively sheds galactomannan and is killed by septum formation inhibitors. *Mol Microbiol* 95:458–471. <https://doi.org/10.1111/mmi.12877>.
 34. Henry C, Latgé J-P, Beauvais A. 2012. α 1,3 Glucans are dispensable in *Aspergillus fumigatus*. *Eukaryot Cell* 11:26–29. <https://doi.org/10.1128/EC.05270-11>.
 35. Gravelat FN, Beauvais A, Liu H, Lee MJ, Snarr BD, Chen D, Xu W, Kravtsov I, Hoareau CMQ, Vanier G, Urb M, Campoli P, Al Abdallah Q, Lehoux M, Chabot JC, Ouimet M-C, Baptista SD, Fritz JH, Nierman WC, Latgé JP, Mitchell AP, Filler SG, Fontaine T, Sheppard DC. 2013. *Aspergillus* galactosaminogalactan mediates adherence to host constituents and conceals hyphal β -glucan from the immune system. *PLoS Pathog* 9:e1003575. <https://doi.org/10.1371/journal.ppat.1003575>.
 36. Samar D, Kieler JB, Klutts JS. 2015. Identification and deletion of Tft1, a predicted glycosyltransferase necessary for cell wall β -1,3;1,4-Glucan synthesis in *Aspergillus fumigatus*. *PLoS One* 10:e0117336. <https://doi.org/10.1371/journal.pone.0117336>.
 37. Komachi Y, Hatakeyama S, Motomatsu H, Futagami T, Kizjakina K, Sobrado P, Ekino K, Takegawa K, Goto M, Nomura Y, Oka T. 2013. gfsA encodes a novel galactofuranosyltransferase involved in biosynthesis of galactofuranose antigen of O-glycan in *Aspergillus nidulans* and *A. fumigatus*. *Mol Microbiol* 90:1054–1073. <https://doi.org/10.1111/mmi.12416>.
 38. Katafuchi Y, Li Q, Tanaka Y, Shinozuka S, Kawamitsu Y, Izumi M, Ekino K, Mizuki K, Takegawa K, Shibata N, Goto M, Nomura Y, Ohta K, Oka T. 2017. GfsA is a β 1,5-galactofuranosyltransferase involved in the biosynthesis of the galactofuran side chain of fungal-type galactomannan in *Aspergillus fumigatus*. *Glycobiology* 27:568–581. <https://doi.org/10.1093/glycob/cwv028>.
 39. Lamarre C, Beau R, Balloy V, Fontaine T, Hoi JWS, Guadagnini S, Berkova N, Chignard M, Beauvais A, Latgé J-P. 2009. Galactofuranose attenuates cellular adhesion of *Aspergillus fumigatus*. *Cell Microbiol* 11:1612–1623. <https://doi.org/10.1111/j.1462-5822.2009.01352.x>.
 40. Engel J, Schmalhorst PS, Routier FH. 2012. Biosynthesis of the fungal cell wall polysaccharide galactomannan requires intraluminal GDP-mannose. *J Biol Chem* 287:44418–44424. <https://doi.org/10.1074/jbc.M112.398321>.
 41. Lussier M, Sdicu A-M, Bussey H. 1999. The KTR and MNN1 mannosyltransferase families of *Saccharomyces cerevisiae*. *Biochim Biophys Acta* 1426:323–334.
 42. Rayner JC, Munro S. 1998. Identification of the MNN2 and MNN5 mannosyltransferases required for forming and extending the mannose branches of the outer chain mannans of *Saccharomyces cerevisiae*. *J Biol Chem* 273:26836–26843.
 43. Sfih-Louaila G, Hurtaux T, Fabre E, Fradin C, Mée A, Pourcelot M, Maes E, Bouckaert J, Mallet J-M, Poulain D, Delplace F, Guéardel Y. 2016. *Candida albicans* β -1,2-mannosyltransferase Bmt3 prompts the elongation of the cell-wall phosphopeptidomannan. *Glycobiology* 26:203–214. <https://doi.org/10.1093/glycob/cwv094>.
 44. da Silva Ferreira ME, Kress MR, Savoldi M, Goldman MH, Härtl A, Heinekamp T, Brakhage AA, Goldman GH. 2006. The akuBKU80 mutant deficient for nonhomologous end joining is a powerful tool for analyzing pathogenicity in *Aspergillus fumigatus*. *Eukaryot Cell* 5:207–211. <https://doi.org/10.1128/EC.5.1.207-211.2006>.
 45. Cove DJ. 1966. The induction and repression of nitrate reductase in the fungus *Aspergillus nidulans*. *Biochim Biophys Acta* 113:51–56.
 46. Girardin H, Latgé JP, Srikantha T, Morrow B, Soll DR. 1993. Development of DNA probes for fingerprinting *Aspergillus fumigatus*. *J Clin Microbiol* 31:1547–1554.
 47. Sezonov G, Joseleau-Petit D, D'Ari R. 2007. *Escherichia coli* physiology in Luria-Bertani broth. *J Bacteriol* 189:8746–8749. <https://doi.org/10.1128/JB.01368-07>.
 48. Clavard C, Beauvais A, Barbin L, Munier-Lehmann H, Latgé J-P. 2012. The composition of the culture medium influences the β -1,3-glucan metabolism of *Aspergillus fumigatus* and the antifungal activity of inhibitors of β -1,3-glucan synthesis. *Antimicrob Agents Chemother* 56:3428–3431. <https://doi.org/10.1128/AAC.05661-11>.
 49. DuBois M, Gilles KA, Hamilton JK, Rebers PA, Smith F. 1956. Colorimetric method for determination of sugars and related substances. *Anal Chem* 28:350–356. <https://doi.org/10.1021/ac60111a017>.
 50. Stalhberger T, Simenel C, Clavard C, Eijnsink VGH, Jourdain R, Delepierre M, Latgé J-P, Breton L, Fontaine T. 2014. Chemical organization of the cell wall polysaccharide core of *Malassezia restricta*. *J Biol Chem* 289:12647–12656. <https://doi.org/10.1074/jbc.M113.547034>.
 51. Morelle W, Faid V, Chirat F, Michalski J-C. 2009. Analysis of N- and

- O-linked glycans from glycoproteins using MALDI-TOF mass spectrometry. *Methods Mol Biol* 534:5–21. https://doi.org/10.1007/978-1-59745-022-5_1.
52. Striebeck A, Robinson DA, Schüttelkopf AW, van Aalten DMF. 2013. Yeast Mnn9 is both a priming glycosyltransferase and an allosteric activator of mannan biosynthesis. *Open Biol* 3:130022. <https://doi.org/10.1098/rsob.130022>.
 53. Hill K, Boone C, Goebel M, Puccia R, Sdicu AM, Bussey H. 1992. Yeast Kre2 defines a new gene family encoding probable secretory proteins, and is required for the correct N-glycosylation of proteins. *Genetics* 130: 273–283.
 54. Hall RA, Gow NAR. 2013. Mannosylation in *Candida albicans*: role in cell wall function and immune recognition. *Mol Microbiol* 90:1147–1161. <https://doi.org/10.1111/mmi.12426>.